Segregated Fermentation Model for Growth and Differentiation of *Bacillus licheniformis*

Andrew P. Fordyce and James B. Rawlings
Dept. of Chemical Engineering, The University of Texas, Austin, TX 78712

This article evaluates the effectiveness of a segregated model for prediction of growth and differentiation of Bacillus licheniformis in a submerged-culture fermentation system. The segregated model accounts for each of the three morphological forms of the Bacillus life cycle. The sporangium biomass was characterized using an age-population model to reflect the age-dependent progress toward spore formation. Constitutive relationships governing the rates of vegetative cell reproduction, spore germination, commitment to sporulation, and substrate consumption are proposed. Based on this model framework, the dynamic cell growth and differentiation equations were developed.

Batch, steady-state and step-test fermentation data from a laboratory-scale fermentor were incorporated into a maximum likelihood parameter estimation scheme for model identification. Confident estimates of growth and differentiation parameters were obtained for the segregated model using biomass measurements. In addition, the model describes successfully growth and differentiation in batch and steady-state operating modes.

Introduction

Products derived from microbial sources have played an important role in the development of our society. In particular, a class of microbial products known as secondary metabolites have found use in a variety of important areas including human and animal medicine, food processing, and industrial chemical processing. The economic significance of secondary metabolites has stimulated efforts toward development of improved operating and control strategies. In fermentation applications, however, the limiting factor in process development is often the level of process understanding, which is usually in the form of a mathematical model. Typically, fermentation systems are difficult to model because of nonlinear dynamics, complex input interactions, and large process time delays. Therefore, to improve process control in secondary metabolite systems, there is a need for accurate, but tractable, fermentation models.

Most efforts toward development of models for secondary metabolite systems have utilized simple unstructured microbial growth and metabolite production models. These unstructured models assume microbes are a single component distributed continuously through the fermentation medium. This oversimplified picture of a fermentation system generally results in an inadequate characterization of growth and secondary metabolite production behavior. In turn, poor process understanding hampers development of process operating and optimization strategies.

In contrast with the unstructured approach's assumption that a fermentation culture is represented as a single component reaction, microorganisms are individual entities consisting of a heterogeneous mixture of many different substances. Further, a single species of microorganism can exhibit multiple morphologies, and often production of secondary metabolites is linked to a specific morphology or to the process of transformation from one form to another. Therefore, for a model to characterize successfully a secondary metabolite fermentation, it is important that the model recognize both the existence of different forms of biomass and the fact that the culture consists of a population of individuals all in different states of growth, differentiation, and production. Models that can account for the existence of different types of biomass and account for the effect of the individual on the cell population are known as structured-segregated models.

Correspondence concerning this article should be addressed to J. B. Rawlings.
Current address of: A. P. Fordyce, Novo Nordisk Biochemical, NA, P.O. Box 576, Franklinton, NC 27525; J. B. Rawlings, Dept. of Chemical Engineering, University of Wisconsin, Madison, WI 53706.

In an effort to explore the utility of the segregated modeling approach, this article presents a structured-segregated model for growth and differentiation of *Bacillus licheniformis*. The *B. licheniformis* fermentation represents a good system to develop a segregated model. First, species from the genus *Bacillus* exhibit a complex life cycle, which includes a sporulation step. In addition, many *Bacillus* species produce sporulation-associated products that are used industrially. *B. licheniformis* produces the peptide-antibiotic bacitracin during sporulation, which is useful in treating infections in surface wounds. Because *B. licheniformis* exhibits different stages of development, and expression of the products of interest is associated with progress into a developmental transformation, a structured-segregated model provides the proper framework for describing the important elements of growth and differentiation and relating them to product expression.

Several researchers have modeled growth, differentiation, and production characteristics of *Bacillus* systems. The first is attributable to Dawes and Thornley (1970), who developed a segregated model to describe growth and sporulation in continuous culture. More recently, sporulation models have been examined by Ollis (1983) and Schulz et al. (1985). Ollis modeled the production of exotoxin from *B. thuringiensis* using an age-structured model. The kinetics of exotoxin production were treated using the Luedeking–Piret equation, and spore formation was considered to be first order with respect to the delayed biomass concentration. Similar to Ollis, Schulz et al. modeled exotoxin production from *B. thuringiensis* using a morphologically structured model with four distinguishable cell states. Transition between the vegetative phase to sporangium, and in turn, to exotoxin-containing cells, and finally mature spores was modeled using delay differential equations. This model was used to characterize batch and continuous growth, and optimal operation was determined for one- and two-stage continuous fermentations.

The highly structured, single-cell models, popularized by the Cornell *E. coli* model of Shuler et al. (1979), have been applied recently to the *Bacillus* species in an attempt to model the differentiation process. Jeong et al. (1990) have proposed a structured single-cell model consisting of 39 nonlinear differential equations with almost 200 parameters. This model attempted to account for the principal interactions between the major metabolic networks in *B. subtilis*, with the goal of describing the biochemical patterns associated with the transition from vegetative growth to sporulation. A similar structured approach has been used by Starzak and Bajpai (1991) to model the vegetative growth cycle and the transition to sporulation.

In this article both batch and steady-state fermentation models are developed for growth and differentiation of *B. licheniformis*. The model consists of a structured description of the three forms of biomass, and an age-population description of the sporangium cells in the process of sporulation. Laboratory fermentation data are utilized to obtain confident parameter estimates for the growth and sporulation kinetics of the *B. licheniformis* system.

Segregated Model Development

An obvious characteristic of a *Bacillus* culture is the presence of three distinct cell types: vegetative, sporangium, and spore. A logical modeling approach is to structure the biomass according to its three distinct morphologies. Morphological structure is appealing because it provides an accurate representation of the actual microscopic picture. Also, since the production of many secondary metabolites is localized in the differentiating portion of the biomass, it is important that a model recognize the existence of the different types of biomass. Based on the Dawes and Thornley (1970) model, this work utilizes a similar morphological structure to develop a dynamic model for *B. licheniformis* in batch and continuous culture modes.

By deciding to structure the *B. licheniformis* system based on cell morphology, a foundation for the proposed model has been established. In addition to the model structure, it is necessary to characterize the level of detail required to model each portion of the biophase. Finally, to complete the model, it is essential that the mechanisms by which the cell groups interact with each other and their environment are identified and characterized.

The interconnected cycles of growth and differentiation exhibited by *B. licheniformis* are diagrammed in Figure 1. Processes including spore germination, vegetative growth, substrate consumption, and sporulation commitment are all involved in the relationships relating cell morphologies, and therefore must be described by the model.

Vegetative biomass model

As noted by Fredrickson (1976), the unstructured Monod model is unable to describe a variety of commonly observed phenomena associated with bacterial batch growth. Batch experiments from this study show the typical growth lag period and postnutrient cell division, both of which are unexplainable using the simple Monod model. To describe effectively transient batch-growth kinetics, a two-compartment chemical model, diagrammed in Figure 2, has been utilized. The structured growth model makes a distinction between the ability of a cell to take up a limiting nutrient, and the capacity to convert that nutrient into biomass. The hypothesis of competitive rates of nutrient transport and biomass production was first proposed by von Bertalanffy (see Tsuchiya et al. (1966),

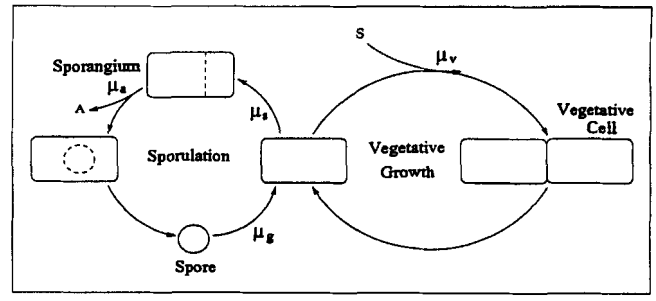

Figure 1. Interconnected cycles of growth and differentiation in *B. licheniformis*.

During the vegetative cycle, substrate, s, is consumed in the process of growth and binary fission. During sporulation, vegetative cells go through a process of transformation that is linked to antibiotic production. The rates of spore germination, vegetative growth, sporulation commitment, and antibiotic production are represented by μ_g, μ_v, μ_s, and μ_a, respectively.

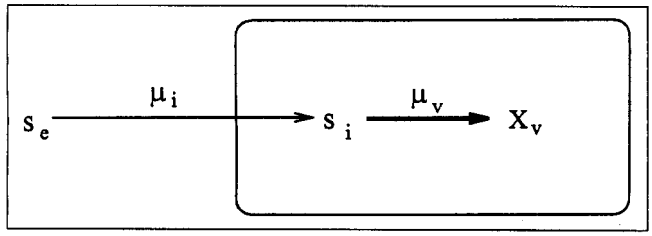

Figure 2. Structured vegetative cell model.

External substrate, s_e, is internalized at a rate μ_i, and converted to readily utilizable biosynthetic precursor, s_i. Cell precursor, s_i, is then converted into new biomass, X_v, at a rate μ_v.

p. 195). Similar two-compartment models have also been proposed by Williams (1967) and Ramkrishna et al. (1967).

Using the structured vegetative model, growth is considered to be a two-stage process. First, the limiting external nutrient is taken up by the existing biomass at a rate given by μ_i. This nutrient exists internally in the cell, represented by s_i, as readily available precursors for biosynthesis and energy production. In the second stage, the internalized nutrient pool is utilized at a rate given by μ_v, to produce biomass and energy necessary for growth and maintenance. Using this approach, the two-compartment growth model effectively describes the initial lag in batch growth and provides a possible explanation for increases in cell number after external nutrient exhaustion.

Utilizing Monod kinetics in the structured growth model gives the following specific substrate internalization and biomass production expressions:

$$\mu_i = \frac{\alpha_i s_e}{K_i + s_e} \tag{1}$$

$$\mu_v = \frac{\alpha_v s_i}{K_v + s_i} - m_v. \tag{2}$$

The resulting equations utilize five adjustable parameters. The parameters α_i and α_v represent the maximum rates of substrate internalization and biomass production, respectively, and K_i and K_v are affinity constants representing the nutrient concentration needed to drive the kinetics at half the maximum rate. Cell death is accounted for using the first-order death constant, m_v.

Spore biomass model

The spore biomass is a source for vegetative cells through the process of germination. Therefore, to provide a complete characterization of the *B. licheniformis* system, it is necessary to develop a rate expression relating germination to the fermentor conditions. However, for most industrial fermentations, spore germination does not contribute significantly to vegetative cell concentrations after the initial inoculant is prepared (Dawes and Thornley, 1970). Also, spore germination experiments carried out for this study indicate that germination is subject to a time delay of 15 h or more (Fordyce, 1992). Observation of a germination time delay is consistent with the findings of other groups. In particular, Marahiel et al. (1979) found that outgrowth in *B. brevis* occurred after an 8–10-h lag period. Also, Dawes and Thornley (1970) considered the number of germinating spores to be insignificant in continuous culture experiments with *B. subtilis*. These results indicate that germination is a relatively slow process compared to growth and sporulation in normal batch and continuous culture. Therefore, the effects of germination are considered negligible in this development. For completeness, model terms for spore germination are included in the modeling equations; however, the rate of germination is set to zero by assuming the specific rate of germination, $\mu_g = 0$.

Sporangium model

There are many morphological and biochemical differences between sporangia at different stages of development. Significantly, many secondary metabolites are produced during sporulation, and the rate of product formation is thought to depend on the progress through the sporulation pathway. Therefore, not only are the sporangia distinguishable based on their progress toward creating a spore, but it is logical that the model should recognize the differences in sporangia if the goal is to predict production of a sporulation-dependent product. This implies the need for a segregated model, which recognizes the differences in sporangia, and allows for incorporation of the distinguishing characteristics of the sporangium population into a production model. Translation of the notion of distinguishability between individuals into a mathematical description involves development of the population balance. The population balance is simply an accounting of individuals in a population as the descriptive characteristics change and individuals enter and leave the group (Ramkrishna, 1979; Randolph and Larson, 1988).

With the purported connection between differentiation and expression of secondary metabolites, a logical characterization of the sporangium population is some measure of progress through the differentiation process. As research into the sporulation process has progressed, it is becoming clear that differentiation in *Bacillus* is a precise sequence of temporally, spatially, and morphologically regulated events (Losick and Kroos, 1989). It appears that the steps of the differentiation process are controlled at the transcriptional level, with each set of genes in the sequence being activated at a specific time in the process (Losick et al., 1986). This strict regulatory pattern forces a close correlation between the biochemical and morphological markers of sporulation and time since commitment to differentiation (Losick and Youngman, 1984; Young and Mandelstam, 1979; Schaeffer, 1969). Therefore, a convenient means to characterize the sporangium population, based on stage of spore development, is the sporangium age, or time since commitment to sporulation.

Let τ represent the sporangium age. Defining $X_s(\tau, t)$ as the sporangium age density function, which is the number of sporangia of age τ at time t per unit volume, the basis of the population balance has been established. Now, the remaining tasks to complete the population balance description are elucidation of mechanisms by which cells enter and leave the population, and a description of how the population changes due to the fact that the distinguishing characteristic, age, changes in time. Selection of cell age as an internal coordinate makes the latter of these two tasks a trivial matter. Cell age is directly correlated with time since birth; therefore, the

rate that cells age, $d\tau/dt$, is a constant of one. Similarly, the choice of cell age as the descriptive characteristic provides a convenient simplification to the modeling of sporangium birth. Since by definition, cells are of age zero at birth, all entries to the population resulting from birth mechanisms are localized at the zero age boundary. Therefore, an understanding of the rate that vegetative cells sporulate is sufficient information to describe the effect of birth on the sporangium population.

Although the regulatory mechanism for control of sporulation initiation is becoming clear, it is difficult to translate the detailed regulatory information into a useful mechanistic model due to the lack of kinetic understanding for the various developmental steps. As was mentioned previously, some researchers are utilizing highly structured models to describe sporulation (Starzak and Bajpai, 1991; Jeong et al., 1990). However, the large number of parameters, and the lack of measurable states brings into question the feasibility of model identification for these single-cell models.

Prior to the single-cell models, work concerning sporulation modeling has depended on empirical approaches to describe sporulation initiation. An example of an empirical approach to model the apparent dependence of sporulation on growth rate was presented by Dawes and Thornley (1970). In their model the specific rate of sporulation, μ_s, was defined to represent the rate of loss of vegetative cells, X_v, due to sporulation:

$$\mu_s = -\frac{1}{X_v}\frac{dX_v}{dt}. \tag{3}$$

Based on observation of steady-state sporulation in *B. subtilis*, Dawes and Thornley postulated a linear relationship between the vegetative growth rate, μ_v, and μ_s:

$$\mu_s = \alpha_s - \beta_s \mu_v. \tag{4}$$

The parameter α_s represents the maximum rate of sporulation and β_s modulates the inhibitory effect of vegetative growth on the rate of sporulation. This relationship shows the decrease in sporulation observed when growth rate is high. The dependence of μ_s on μ_v provides an implicit dependence of sporulation on limiting substrate concentration through Eq. 2.

Dawes and Thornley were able to represent accurately steady-state sporulation data for *B. subtilis* using the linear relationship in Eq. 4. However, batch experimental data in combination with dilution-rate step tests indicate that the linear relationship does not hold when limiting substrate concentration approaches zero (Fordyce, 1992). Therefore, instead of assuming a linear relationship between growth and sporulation, an experimentally fit, piecewise-linear expression has been utilized to model the dependence of sporulation commitment, μ_s, on limiting substrate concentration. In a general formulation, the empirical sporulation function can be represented by

$$\mu_s = \sum_{j=1}^{n} \gamma_j \phi_j(s_i), \tag{5}$$

where ϕ_j represents the jth piecewise linear basis function, and γ_j is a model parameter representing the rate of sporulation at the jth node. Unlike the assumption of linear dependence of sporulation on growth rate, utilization of the elemental approximation for the dependence of sporulation on limiting internal substrate has proved effective in describing sporulation commitment during both steady-state and transient growth.

Along with the description of the sporangium birth through sporulation initiation, an understanding of the mechanisms by which cells leave the population is required to complete the population description. For this study, it is assumed that there is no significant loss of cells resulting from death of sporangia. There is, however, a mechanism by which sporangia leave the population. At the conclusion of the sporulation process, cells have been completely transformed from the vegetative state to dormant spores. Therefore, by definition, the maturation time represents a division between the sporangium population and the unstructured spore state.

While the point where a sporangium cell has truly reached maturity is somewhat arbitrary, for the purposes of this research it is defined to be the stage of development where sporangia acquire heat resistance. Based on the assumption that spore development occurs in a fixed amount of time, the age of spore maturation is defined as τ_m. The period required for *B. subtilis* to achieve maturity has been estimated by several researchers to be in the range of 8 to 10 h (Nicholson and Setlow, 1990; Losick and Youngman, 1984). Recognizing that the true time of spore maturation is vague, and to account for any species-related differences between *B. licheniformis* and *B. subtilis*, τ_m has been treated as an adjustable parameter that is insensitive to changes in culture conditions.

The rates of sporulation commitment and spore maturation, in combination with the microscopic continuity equation, give the age-dependent population balance:

$$\frac{\partial X_s}{\partial t} + \frac{\partial X_s}{\partial \tau} = \delta(\tau)\mu_s X_v - \delta(\tau - \tau_m)X_s. \tag{6}$$

The Dirac delta functions associated with birth and death account for the fact that the processes of sporulation commitment and maturation act as a point source and sink, respectively.

Segregated fermentation model

Dynamic Equations. The dynamic segregated fermentation model is developed by coupling the kinetic expressions for the various rate processes to the fluid dynamics model for the fermentation apparatus of interest. In this study, a stirred-tank fermentation reactor has been utilized, and in the development of the segregated model equations assumptions include constant fluid density, perfect mixing, constant temperature, single-substrate-limited rate processes, and sterile feed.

Based on a continuous-stirred-tank fermentor of liquid volume V_r, the modeling equations are formed by performing material balances on spore and vegetative cell concentrations, limiting substrate concentration, fermentor mass, and sporangium-cell number density. The resulting coupled inte-

Table 1. Definitions of State and Independent Variables for the Age-Segregated Fermentation Model

Variable	Dimensionless Definition	Description
t	$\hat{t} = t/\tau_m$	Time (h)
τ	$\hat{\tau} = \tau/\tau_m$	Sporangium age (h)
X_e	$\hat{X}_e = \dfrac{X_e}{y_v s_{e0}}$	Endospore concentration (cells/L)
X_v	$\hat{X}_v = \dfrac{X_v}{y_v s_{e0}}$	Vegetative cell concentration (cells/L)
s_e	$\hat{s}_e = \dfrac{s_e}{s_{e0}}$	External substrate concentration (g/L)
s_i	$\hat{s}_i = s_i y_v$	Internal substrate concentration (g/cell)
$X_s(t, \tau)$	$\hat{X}_s = \dfrac{X_s \tau_m}{y_v s_{e0}}$	Sporangium number density (cells/(L·h))
V_r	$\hat{V}_r = \dfrac{V_r}{V_{r0}}$	Working reactor volume (L)
D	$\hat{D} = \dfrac{F\tau_m}{V_r}$	Dilution rate (1/h)

grodifferential equations make up the dynamic segregated fermentor model. For convenience, the state and independent variables, with their dimensionless definitions, are summarized in Table 1. The specific kinetic rate functions are described in Table 2.

With a circumflex (hat) over a variable representing a dimensionless state, the model is presented in dimensionless form:

Spore Biomass

$$\frac{d\left(\hat{X}_e\hat{V}_r\right)}{d\hat{t}} = \hat{\delta}(\hat{\tau}-1)\hat{X}_s\hat{V}_r - \hat{\mu}_g\hat{X}_e\hat{V}_r - \frac{F_o\tau_m}{V_{r0}}\hat{X}_e. \quad (7)$$

Vegetative Biomass

$$\frac{d\left(\hat{X}_v\hat{V}_r\right)}{d\hat{t}} = (\hat{\mu}_v - \hat{\mu}_s)\hat{X}_v\hat{V}_r + \hat{\mu}_g\hat{X}_e\hat{V}_r - \frac{F_o\tau_m}{V_{r0}}\hat{X}_v. \quad (8)$$

External Substrate

$$\frac{d(\hat{s}_e\hat{V}_r)}{d\hat{t}} = \frac{F_i\tau_m}{V_{r0}}\hat{s}_f - \hat{\mu}_i\hat{X}_v\hat{V}_r - \frac{y_v}{y_g}\hat{\mu}_g\hat{X}_e\hat{V}_r - \frac{F_o\tau_m}{V_{r0}}\hat{s}_e. \quad (9)$$

Table 2. Kinetic Rate Variables for the Age-Segregated Fermentation Model

Function	Dimensionless Definition	Description
μ_g	$\hat{\mu}_g = \mu_g\tau_m$	Endospore germination rate (1/h)
μ_i	$\hat{\mu}_i = \mu_i y_v \tau_m$	Substrate internalization rate (g/cell·h)
μ_s	$\hat{\mu}_s = \mu_s\tau_m$	Sporulation rate (1/h)
μ_v	$\hat{\mu}_v = \mu_v\tau_m$	Vegetative growth rate (1/h)

Internal Substrate

$$\frac{d\left(\hat{s}_i\hat{X}_v\hat{V}_r\right)}{d\hat{t}} = \hat{\mu}_i\hat{X}_v\hat{V}_r - \left(\hat{\mu}_v + \frac{y_v}{y_s}\hat{\mu}_s\right)\hat{X}_v\hat{V}_r - \frac{F_o\tau_m}{V_{r0}}\hat{s}_i\hat{X}_v. \quad (10)$$

Culture Volume

$$\frac{d\hat{V}_r}{d\hat{t}} = (F_i - F_o)\frac{\tau_m}{V_{r0}}. \quad (11)$$

Sporangium Number

$$\frac{\partial\left(\hat{X}_s\hat{V}_r\right)}{\partial\hat{t}} = -\frac{\partial\hat{X}_s}{\partial\hat{\tau}}\hat{V}_r + \hat{\delta}(\hat{\tau})\hat{\mu}_s\hat{X}_v\hat{V}_r - \hat{\delta}(\hat{\tau}-1)\hat{X}_s\hat{V}_r - \frac{F_o\tau_m}{V_{r0}}\hat{X}_s. \quad (12)$$

Equations 7–11 represent the dynamic ordinary differential equations (ODEs) modeling the nonsegregated vegetative and endospore cell populations, along with the substrate and culture volume material balances. Equation 12 is a balance on the sporangium cell number, resulting in a hyperbolic partial differential equation (PDE) representing the change in number of sporangium cells of age, τ, at time t. The sporangium cell balance is coupled to the vegetative cell balance through sporulation initiation, which is treated as a point birth source in Eq. 12. Maturation of sporangia couples the sporangium population balance to the endospore balance, appearing as the input term, $\hat{\delta}(\hat{\tau}-1)\hat{X}_s$, in Eq. 7. For convenience, the dimensionless hat notation will be dropped, and all equations are presented in dimensionless form unless otherwise noted.

Complete analytical solutions of the resulting segregated dynamic modeling equations are generally not possible due to the nonlinear nature of the problem. Therefore, development of a numerical technique is necessary for solution of the fermentor model. Fortunately, efficient computer codes exist for the solution of nonlinear ODEs (Brenan et al., 1989). The population balance, which is a PDE, adds a degree of complexity to the problem. In fact, efficient solution of the PDE is the crux of the numerical solution task.

While a variety of numerical techniques exist for solution of PDEs, the hyperbolic nature of the population balance leads to propagation of discontinuities along characteristic lines in the domain, creating difficulties when using standard finite-difference and method of weighted residuals techniques (Lapidus and Pinder, 1982). However, the linear structure of the age-population balance allows for a semianalytical solution of Eq. 12:

$$X_s(t,\tau)V_r(t) = X_s(t-\tau,0)V_r(t-\tau)\exp\left[-\int_{t-\tau}^{t}\frac{F_o(s)}{V_r(s)}ds\right]. \quad (13)$$

To utilize the semianalytical solution, $X_s(t, \tau)$ is approximated by a linear combination of polynomial basis functions

in τ with time-varying coefficients:

$$X_s(t,\tau) \approx \sum_{i=0}^{n} \gamma_i(t) L_i(\tau). \tag{14}$$

The function can be represented equivalently, and more conveniently, in terms of its values $X_{s_i}(\tau_i)$ at n points, (τ_i, ... , τ_n), in the domain, known as collocation points (Villadsen and Stewart, 1967). The $L_i(\tau)$ polynomials are chosen such that they are orthogonal to each other on the problem domain, and the collocation points are chosen to be the $n+1$ roots of the $L_{n+1}(\tau)$ polynomial.

Discretization of the population balance equation reduces the dynamic fermentation model to a set of nonlinear ODEs. While it is currently not possible to solve general nonlinear differential equations analytically, a variety of numerical integration packages exist for the solution of coupled nonlinear ODEs. Therefore, the dynamic fermentation model has been reduced to a numerically tractable form (Fordyce, 1992).

Steady-State Equations. Steady-state operation of a continuous-stirred-tank fermentor involves continuous feed of nutrient medium, accompanied by continuous removal of fermentation broth. Continuous operation of a fermentor, known as chemostat operating mode (Bailey and Ollis, 1986), is a useful technique for assessing organism behavior in constant environmental conditions. In this study, steady-state experiments have been utilized to gain information for estimation of model parameters. Therefore, a steady-state formulation of the segregated model is required to predict the steady-state behavior of the *B. licheniformis* system.

The steady-state behavior of the segregated fermentation model is represented by the fixed points of the dynamic equations. Therefore, the steady-state model is formed by substituting zero for all time-dependent terms in the dynamic model. Since the reactor volume is constant, along with the flow into and out of the fermentor, it is convenient to define the operating parameter, $D = F/V_r$ (units of inverse time) known as the dilution rate. Substitution of 0 for the time-dependent terms, and introduction of D into the dynamic modeling equations gives the steady-state model (presented in dimensionless form, where dimensionless $\hat{D} = F_o\tau_m/V_r$):

$$0 = \delta(\tau-1)X_s - \mu_g X_e - DX_e \tag{15}$$

$$0 = (\mu_v - \mu_s)X_v + \mu_g X_e - DX_v \tag{16}$$

$$0 = D(s_f - s_e) - \mu_i X_v - \frac{y_v}{y_g}\mu_g X_e \tag{17}$$

$$0 = \mu_i - \left(\mu_v + \frac{y_v}{y_s}\mu_s\right) - Ds_i \tag{18}$$

$$0 = -\frac{dX_s}{d\tau} + \delta(\tau)\mu_s X_v - \delta(\tau-1)X_s - DX_s. \tag{19}$$

At steady state, the fermentor conditions are time invariant, and the dynamic modeling equations are reduced from a set of coupled ODEs and PDEs to a set of algebraic equations coupled to a differential equation representing the population balance.

Similar to the dynamic-model solution, the nonlinear nature of the fermentation model precludes a general analytical solution for the steady-state case. However, at steady state there is a simple semianalytical solution to the sporangium-age-distribution equation. Integration of Eq. 19 with respect to sporangium age and substitution of the steady-state sporulation initiation expression gives the semianalytical, steady-state sporangium-age density:

$$X_s(\tau) = \mu_s X_v \exp[-D\tau]. \tag{20}$$

This equation reflects the fact that the sporangium number density decreases exponentially with increasing sporangia age at steady state due to the increased probability that a cell will wash out of the fermentor as it ages.

As with the dynamic model, the analytical solution to the population balance is utilized by discretizing the age-dependent sporangium density, and expanding the steady-state number density as orthogonal polynomials in τ. Representing the steady-state distribution in terms of its value at the collocation points reduces the steady-state sporangium distribution to a set of algebraic equations:

$$X_{s_i}(\tau_i) = \mu_s X_{v_s} \exp[-D\tau_i]. \tag{21}$$

Similar to the dynamic case, general analytical solutions to the steady-state model are not possible; however, a variety of algorithms exist to solve sets of nonlinear algebraic equations.

Segregated Model Identification

Considering the lack of *a priori* knowledge concerning the segregated model parameters, fermentation data are required to identify and validate the proposed model. Therefore, batch and continuous fermentation data have been collected for the *B. licheniformis* fermentation. Based on these data, sensitivity analysis and a maximum-likelihood estimator have been utilized to identify the segregated-model parameters. These data are also used to examine the usefulness of the segregated model in a wide range of operating conditions.

Like many fermentation applications, not all model states are readily measurable. The segregated model structures the biomass into three morphological phases—vegetative, sporangium, and spore—each with distinct physical characteristics. However, using available measurement techniques, it was not possible to measure the distribution of the biomass in the three phases. Further, the age-distribution characteristics of the sporangium population were also not measured. The only readily available technique to characterize the biomass is to utilize the heat-resistant properties of the spores to distinguish between spore and nonspore biomass. In addition to the biomass measurements, the concentration of the limiting substrate, glucose, concentration was measured. The resulting outputs for the segregated model are given by

$$y_{\text{spo}} = X_e \tag{22}$$

$$y_{\text{nspo}} = X_v + \int_0^{\tau_m} X_s \, d\tau \tag{23}$$

$$y_{sub} = s_e. \tag{24}$$

As the output equations show, the biomass outputs are the spore concentration and a combination of the vegetative and total sporangium cell concentrations.

Experimental methods

Data for this study were collected using a New Brunswick Multigen Model F-2000 fermentor with a 2.0-L batch/continuous fermentation vessel (1.0-L working volume). The fermentation apparatus was equipped with temperature, agitation, pH, and aeration control functions. Fermentation conditions were as follows: temperature 37°C, pH maintained at 7.0 using 1.0 M KOH, agitation rate 400 rpm, aeration rate 1.5 V/(V·min).

The fermentation broth and feed mix recipe were obtained from Hanlon and Hodges (1981) and consisted of the following: glucose (0.15–0.27 wt. %), NH_4Cl 0.01 M, $Na_2HPO_4 \cdot 12H_2O$ 0.04 M, KH_2PO_4 0.026 M, $MgSO_4 \cdot 7H_2O$ 5.0×10^{-4} M, $CaCl_2 \cdot 6H_2O$ 1.0×10^{-4} M, $FeSO_4 \cdot 7H_2O$ 1.0×10^{-5} M, $MnCl_2 \cdot 4H_2O$ 1.0×10^{-5} M. The medium was prepared in two stages. First, phosphate buffering components and the nitrogen source were dissolved in distilled-deionized water and sterilized using steam autoclaving at 121°C. The glucose and metal salts were dissolved as a concentrated solution in distilled-deionized water and sterile filtered using a 0.22-μm filter. This solution was added to the cooled phosphate-buffered components.

Inoculum Preparation. Using a sterile loop, a small quantity of *B. licheniformis* (ATCC 10716) was transferred from a master culture (stored at −70°C in 20% glycerin–water solution) to 5.0 mL of sterile minimal fermentation medium in a foam-capped tube. The tube was incubated in a 37°C shaker bath for 12 h. At that point 1.0 mL of broth was used to inoculate 50 mL of sterile minimal medium in a 250-mL Erlenmeyer flask. This flask was incubated for 12 h in a 37°C shaker bath. To seed batch and continuous fermentations in the 2.0-L minifermentor a 10-mL sample of the shake-flask broth was aseptically transferred to the sterilized fermentation vessel.

Biomass Assays. To assess levels of spore and nonspore biomass in fermentation cultures measurements of the number densities of cells were taken. A 5.0-mL sample of fermentation broth was divided into two volumes, each retained in a sterile test tube. One sample was submerged in an 80°C water bath for 10 min, which was assumed to kill all cells except for mature spores (Nicholson and Setlow, 1990). The other sample was retained at room temperature. After heat treatment, both the heated and unheated samples were serially diluted using sterile deionized water. Samples from several dilutions were plated into cooled LB soft agar (Luria-Bertani broth 2% (Difco), gum agar 0.5% (Sigma)). Plates were incubated at 37°C for at least 12 h prior to counting. Number densities were based on two replicate plates for the dilution where the colony count was between 20 and 200 colony-forming units. Spore number densities were based on the heat-treated colony counts, and nonspore biomass number density was computed as the difference between the non-heat-treated and the heat-treated colony counts.

Substrate Assay. To determine levels of the limiting carbon substrate, glucose, samples of the fermentation broth were centrifuged (5,000×g, 6 min) then stored in a laboratory freezer for analysis at a later date. After completion of a fermentation experiment, samples were thawed and glucose levels were assayed using an immobilized-enzyme glucose analyzer (Yellow Springs Instruments, Model 23A Analyzer).

Batch growth experiments

As an initial step toward estimation of the model parameters, biomass number concentration and substrate concentration were tracked during batch fermentation at 1.5 v/(v·min) aeration. The fermentor was charged with sterile minimal medium, and then innoculated with vegetative cells of *B. licheniformis*. The batch fermentation is typified by a slight delay between inoculation and rapid growth of vegetative cells. Concomitant to the growth phase, substrate is consumed and becomes completely depleted at about 12 h into the run. After substrate is depleted, the nonspore biomass begins to fall. Also associated with substrate exhaustion is the appearance of spores approximately 10 h after the nonspore biomass peaks.

To test the effectiveness of the dynamic model in describing batch fermentation, a maximum-likelihood estimator was used to determine the model parameters using the data from a typical batch fermentation (Bard, 1974). The corresponding fit of the model to the data is shown in Figure 3. The model successfully predicts a lag period, and also allows for the peak nonspore biomass levels to be reached after external substrate is exhausted. The structured vegetative growth model allows for an accurate description of the nonspore biomass, while also successfully tracking the rapid decline in the external substrate. In addition, by providing a mechanism to account for cell death, the model tracks the rapid decline in nonspore biomass, without a large rise in spore biomass. The model is able to account for the delayed spore appearance by explicitly accounting for the delay between sporulation initiation and production of a mature spore.

Although it has been shown that the model can describe batch-growth kinetics, it is important to evaluate the sensitivity of the model to the parameters and to determine the rela-

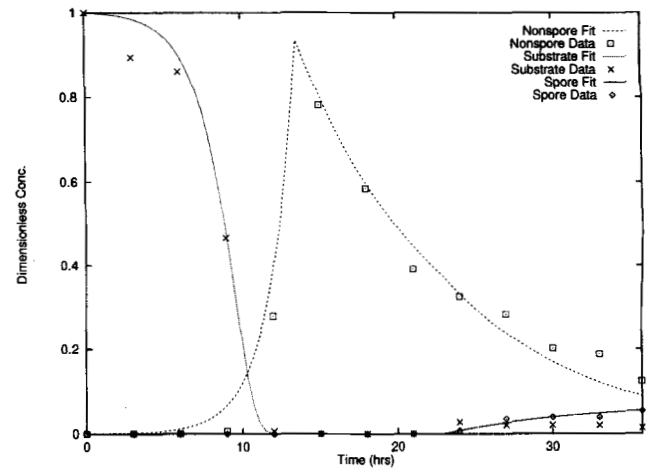

Figure 3. Segregated model fit to batch-fermentation data.

tive confidence of the parameter estimates. Further, since the goal is to develop a model that describes the fermentation system in as wide an operating range as possible, one cannot be satisfied with a model fit to a single batch fermentation. The repeatability of the system for a given experiment must be assessed, along with the ability of the model to simultaneously describe data from different regions of the operating space.

As a first step in analyzing the ability of the model to describe the fermentation, sensitivity analysis has been used to determine which parameters have a significant effect on the model solution. The sensitivity information is useful because the estimation problem can be reduced by setting the insensitive parameters to reasonable values and considering them fixed, thereby minimizing the number of adjustable parameters. However, in using sensitivity analysis to eliminate parameters from the adjustable set, it must be kept in mind that the relative sensitivity of the model with respect to a parameter can be a function of the operating conditions. Therefore, as experimental conditions vary, parameters that had little effect on the model for prior experiments can become significant in the new region of the operating space. Therefore, the assumption of insensitivity for the nonadjustable parameters must be reevaluated as operating conditions change. Further, the issue of output sensitivity must be considered. A given parameter can have a large effect on a model; however, if the outputs are insensitive to the parameter of interest, then the significance of the parameter can go unnoticed.

For the batch experiment, the significant parameters have been determined by perturbing the nominal parameter set and evaluating the change in the solution based on the perturbation. If a parameter perturbation causes a significant change in the model solution it is considered a significant parameter, and it is kept in the set of adjustable parameters. Those parameters that result in an insignificant change when perturbed are considered insensitive, and are removed from the adjustable set.

The sensitivity of the segregated model to the nominal parameters has been determined by perturbing each parameter by $\pm 10\%$. The perturbation analysis shows that the segregated model is insensitive to several parameters during batch operation. The insensitive parameters include, α_i, K_i, K_v, and the rates of sporulation commitment at nonzero substrate concentrations γ_j, $j = 2, \ldots, n$. The insensitivity of the batch model to these parameters is typified by the insignificant change in the model solution in response to perturbations in the maximum rate of substrate uptake, α_i, shown in Figure 4. In contrast, the batch model solution exhibits sensitivity to the remaining growth and differentiation parameters, α_v, m_v, γ_1, and τ_m. The effect of a perturbation in a sensitive parameter is typified by the change in the batch-model solution for changes in α_v, shown in Figure 5.

Utilizing the initial batch fermentation to establish a reasonable set of parameters, and sensitivity analysis to determine the adjustable parameters, the repeatability of the batch fermentation was tested using a replicate batch fermentation. With the fixed parameters set to values based on the first fermentation, the adjustable parameters were reestimated using the second set of data, both using the second fermentation alone and using both sets of data together in one estimation run. The resulting maximum-likelihood parameter esti-

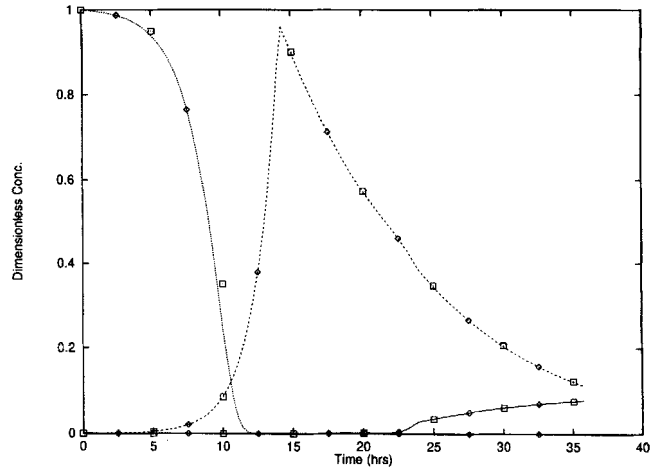

Figure 4. Insensitivity of the segregated model to 10% perturbations in the maximum rate of substrate internalization, α_i.

The nominal spore, nonspore, and substrate profiles are given by the solid, dashed, and dotted lines, respectively. The symbol ◇ represents solution with 10% increase in α_i, and □ is the model solution with a 10% decrease in α_i.

mates for each case, with 2σ confidence intervals, are shown in Table 3. Additionally, the estimates of the measurement error variances for the biomass number concentration and external substrate concentration are also listed.

Estimates for the adjustable parameters are reasonably close between runs. Also, the confidence intervals reflect the overlap between replicate runs, indicating a reasonable degree of repeatability.

The batch experiment provides reasonable sensitivity to the maximum rate of vegetative growth, α_v, yielding an estimate with confidence intervals of less than 10% of the parameter magnitude. The estimated maximum growth rate of 0.717

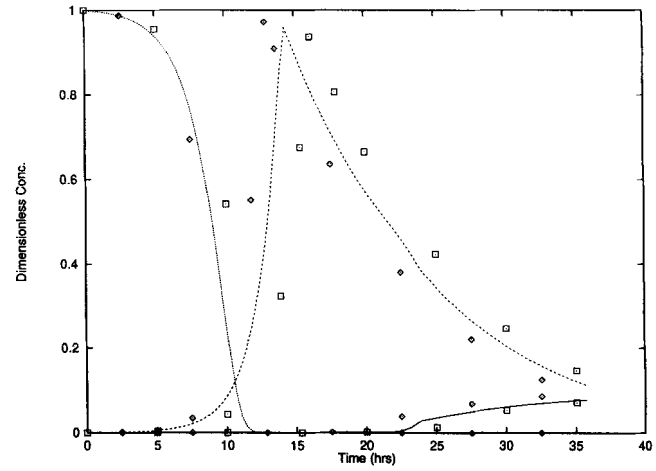

Figure 5. Response of the batch model to 10% perturbations in the maximum rate of vegetative growth, α_v.

The nominal spore, nonspore, and substrate profiles are given by the solid, dashed, and dotted lines, respectively. The symbol ◇ represents the model solution with 10% increase in α_v, and □ is the model solution with a 10% decrease in α_v.

Table 3. Maximum Likelihood Parameter Estimates and Measurement Error Variance Estimates Based on Individual Replicate Batch Experiments: Trial 1 and Trial 2, and Based on Combined Results

Fixed Parameters		
Vegetative growth Michaelis constant	K_v	9.06×10^{-15} (g/cell)
Maximum substrate internalization	α_i	1.01×10^{-12} (g/cell·h)
Internalization Michaelis constant	K_i	1.17 (g/L)
Sporulation commitment coefficients	$\gamma_j, j=2, \ldots, n$	0.0
Sporulation yield coefficient	y_s	∞ (cells/g)

Batch Run	Growth Parameter Estimates		
	α_v (1/h)	m_v (1/h)	$y_v\times10^{-12}$ (cells/g)
Trial 1	0.698 ± 0.009	0.104 ± 0.017	1.015 ± 0.718
Trial 2	0.769 ± 0.117	0.183 ± 0.056	1.308 ± 0.420
Combined	0.717 ± 0.027	0.117 ± 0.020	1.190 ± 0.244

Batch Run	Sporulation Parameter Estimates	
	γ_1 (1/h)	τ_m (h)
Trial 1	0.008 ± 0.003	9.68 ± 0.57
Trial 2	0.023 ± 0.015	9.32 ± 1.00
Combined	0.010 ± 0.007	8.59 ± 0.41

Batch Run	Measurement Error Variances*		
	v_{spo}	v_{nspo}	v_{sub}
Trial 1	1.31×10^{-5}	2.18×10^{-3}	9.46×10^{-4}
Trial 2	1.25×10^{-4}	4.04×10^{-3}	7.98×10^{-4}
Combined	1.11×10^{-4}	5.32×10^{-3}	1.14×10^{-3}

*Variances are reported in dimensionless form.

(1/h) corresponds to a doubling time of 58 min, which matches well with previously reported doubling times ranging from 50 to 90 min for *B. licheniformis* grown aerobically in glucose medium (Donohue and Bernlohr, 1978; Kramer, 1990).

A comparison of the estimated maximum vegetative growth rate to the maximum rate of substrate internalization indicates that once sufficient biosynthetic capacity is built up, the vegetative growth capacity is limiting compared to the rate of substrate internalization. Because of the addition of the internal substrate state, the model is able to describe the growth lag, and postexternal-nutrient exhaustion growth. However, since this structured growth formulation is empirical, phenomenological conclusions concerning the relative rates of bacterial metabolic processes are not justified.

Similar to vegetative growth, the batch experiment provides sensitivity to the cell death rate parameter, m_v. Based on the modified Monod growth law, shown in Eq. 2, the critical internal substrate concentration needed to prevent cell death can be derived:

$$s_{i_{crit}} = \frac{m_v K_v}{\alpha_v - m_v}. \tag{25}$$

For a death rate of 0.117 (1/h), the critical internal substrate concentration, s_i, is 2.84 (g/L), based on a nominal cell volume of 0.62 μm^3. This leads to an equilibrium value of 0.14 (g/L) external substrate concentration, s_e, needed to sustain the internal substrate concentration at the critical level. Therefore, according to the parameters obtained through the batch experiment, the vegetative biomass is able to maintain viability down to low concentrations of the limiting substrate, indicating the effectiveness of glucose as a carbon and energy source.

The 95% confidence intervals for vegetative yield, y_v, and maximum rate of sporulation, γ_1, are not as tight as the growth and death intervals, ranging from approximately 70% of the parameter magnitude for the maximum rate of sporulation to 20% for the vegetative yield coefficient. This indicates that the batch fermentation provides less information for the estimation of these parameters, and this is reflected in the larger confidence intervals.

To gauge whether the sporulation parameters estimated using batch fermentation Trial 1 are reasonable, it is useful to compare these estimates to previously reported parameters. Based on steady-state *B. subtilis* experiments, Dawes and Thornley (1970) report a maximum sporulation rate of $\alpha_s = 0.091$ (1/h), and spore maturation time of 4.0 h. The Dawes and Thornley values for the maximum specific rate of sporulation initiation parameter is an order of magnitude higher than the value 0.010 (1/h) found from the *B. licheniformis* batch data in this study. It is not clear if this discrepancy results from differences between the species studied, differing operating conditions, or if sporulation kinetics differ significantly between batch and steady-state operation. A further discrepancy between the batch results and previously reported data is the estimate of the spore maturation time, with the maturation time of 8.59 h found from the batch data being more than double the value of 4.0 reported by Dawes and Thornley. A potential explanation of the differences between the two estimated maturation times is that Dawes and Thornley used cell refractility as an indication of maturation compared to heat resistance as the maturation marker in this study. Other possible explanations could be related to differences in species and culture conditions.

Comparison of the parameter estimates from the two replicate batch runs shows only a slight degree of variability between runs, and the model does an adequate job of describ-

ing the data. Estimation of the parameters that are sensitive to the batch experiment leads to reasonable confidence limits for the current set of adjustable parameters. However, it is important to realize that repeatability for given operating conditions does not guarantee that the model can represent the system for a wide region of the operating space. It must also be pointed out that the model parameters that have been considered "fixed" merely reflect the fact that the batch fermentations are not sensitive to those parameters. This does not mean that operating conditions through which the previously insensitive parameters become significant do not exist. Of particular concern is the limited confidence the batch experiments provide about the dependence of sporulation initiation on substrate concentration. Estimation of the sporulation parameters based on the batch data provides adequate confidence in the zero substrate sporulation rate, γ_1. However, there is little information concerning attenuation of the sporulation rate as substrate concentration increases. Since the batch experiments were insensitive to the parameters representing the rate of sporulation for nonzero substrate, these parameters were fixed at zero. However, since sporulation phenomena are considered significant with respect to secondary metabolism, it is important that the model's ability to describe these phenomena is tested.

In an effort to better explore the sporulation kinetics exhibited by *B. licheniformis*, experimental data that are more sensitive to the rate of sporulation at nonzero substrate concentration are needed. In an attempt to characterize sporulation, Dawes and Thornley (1970) used continuous-feed step-test experiments to evaluate the spore maturation time for *B. subtilis*. In a similar fashion, step-test experiments have been carried out in this study in an effort to gain information concerning the sporulation dynamics of *B. licheniformis*.

The step-test experimental data were obtained by running the fermentor as a chemostat, with continuous feed of sterile nutrient medium, accompanied by continuous removal of fermentation broth. After achieving steady state at a high feed flow rate and high aeration, a step down in dilution rate was made at time zero. Then the response of the spore concentration to the step down in dilution rate was monitored by periodic sampling of the continuous fermentor. The resulting dynamic spore-concentration profiles for replicate step experiments at high aeration are shown in Figure 6. For these experiments, steady state was achieved for $D = 0.5$ (1/h), and at time zero, the flow rate was stepped down to $D = 0.1$ (1/h).

Prior to making the step down in dilution rate, the fermentor achieved a nontrivial steady state. Assuming that germination is negligible, steady state is achieved when the apparent vegetative growth rate is equal to the dilution rate:

$$\mu_{\text{app}} = \mu_v - \mu_s = D. \tag{26}$$

For the noninhibitory substrates, as the dilution rate increases, the steady-state substrate concentration increases, allowing for an increase in the apparent growth rate to match the dilution rate. Activation of the sporulation pathway becomes more likely as substrate limitations slow growth. Using this reasoning, the higher the dilution rate, the higher the substrate concentration, and therefore the lower the rate of sporulation initiation. This analysis implies that the steady-state spore concentration is low at high dilution rates, and

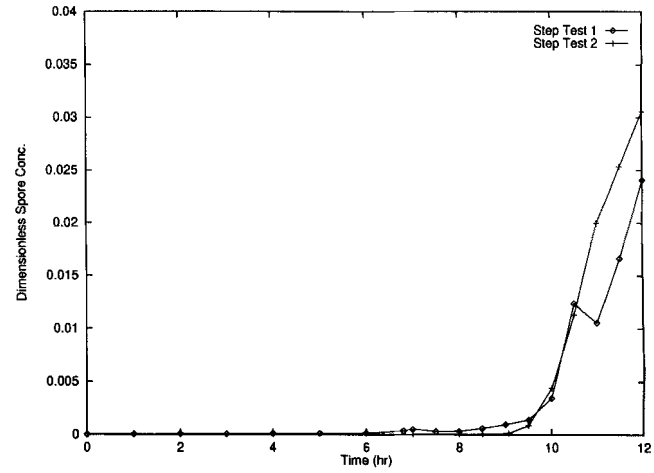

Figure 6. Replicate dimensionless spore concentration profiles in response to a step down in dilution rate from steady state at $D = 0.5$ (1/h) to $D = 0.1$ (1/h).

would be expected to rise as dilution rate is lowered. The dynamic spore profiles, shown in Figure 6, exhibit the expected behavior. At time zero, the system is at steady state, and due to the high dilution rate, the spore concentration is very low. The system responds to the step down in dilution rate with a gradually increasing spore concentration, until approximately 9 h, when a sudden increase in the spore count occurs. The delay prior to the appearance of increased spore counts can be attributed to two effects. Immediately after the step change, a period of time passes where the major system dynamics are the adjustment of the substrate concentration to the reduced feed rate. After substrate concentration falls, the biomass responds with a reduced growth rate, and a significant increase in the rate of sporulation. At that point, the delay of the spore appearance is the maturation lag, τ_m, resulting from the time required for a vegetative cell to differentiate into a spore.

Compared to the batch experiments, the operating conditions used for the step-test experiment create a situation in which the substrate dependence of the sporulation initiation dynamic is more apparent, as is the maturation time. To take advantage of the additional experimental information yielded from the dilution-step experiment, the data from step test 1 were added to the parameter estimation routine, and the growth and sporulation parameters were reestimated using both the batch and step-test data.

For five sporulation parameters (four linear elements), the optimal sporulation initiation function, with the 2σ error bars, is shown in Figure 7. The step-test model fit to the data is shown in Figure 8. The confidence limits on the sporulation rate parameters reflect the sensitivity of the batch and step-test fermentations to particular ranges of substrate concentrations. In the batch experiment, substrate is quickly exhausted, and therefore the data are most sensitive to the rate of sporulation commitment as $s_i = 0$. For this reason, the estimator is relatively confident in the parameter estimate for μ_s at $s_i = 0$. However, the step-test data, using continuous substrate feed, create an experiment that is sensitive to a narrow range of substrate concentrations around $s_i = 0.01$.

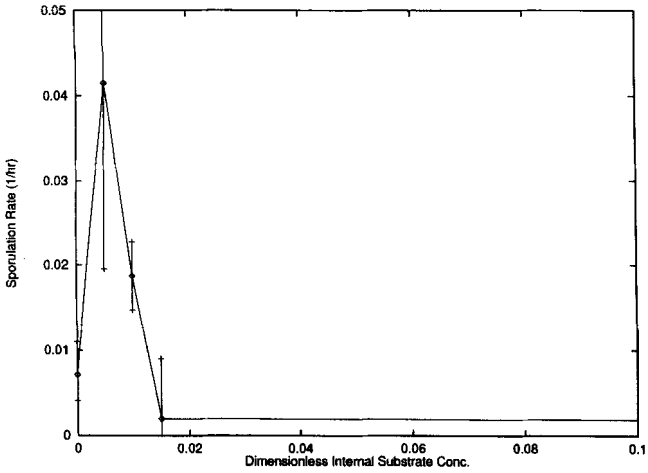

Figure 7. Estimated sporulation initiation function for 4 linear elements concentrated near $s_i = 0$.

The points represent the estimated value of the sporulation function at the element boundaries, and the vertical lines represent the 2σ confidence intervals for estimated rate at each element boundary.

Therefore, these experiments provide better data for estimating the shape of the sporulation function in the substrate region around $s_i = 0.01$. Both the batch and step-test fermentations are insensitive to substrate concentrations just above exhaustion, and therefore this region has larger confidence limits.

Steady-state fermentation experiments

To test the ability of the model to describe steady-state behavior of the *B. licheniformis* fermentation, growth and differentiation data have been collected. Steady state was obtained by running the fermentor initially in batch mode, and after approximately 12 h a continuous metered stream of sterile medium was fed to the fermentation vessel. Samples of fermentation broth were removed periodically from the vessel and biomass and substrate assays were conducted to determine spore, nonspore, and substrate concentration lev-

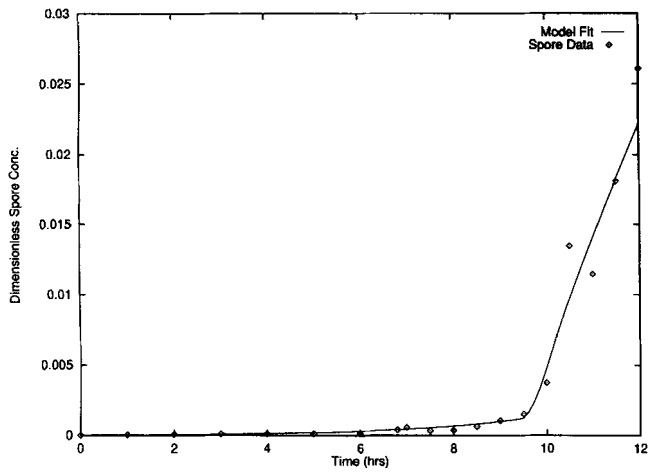

Figure 8. Model fit of the 4 element sporulation initiation function to Step Test 1.

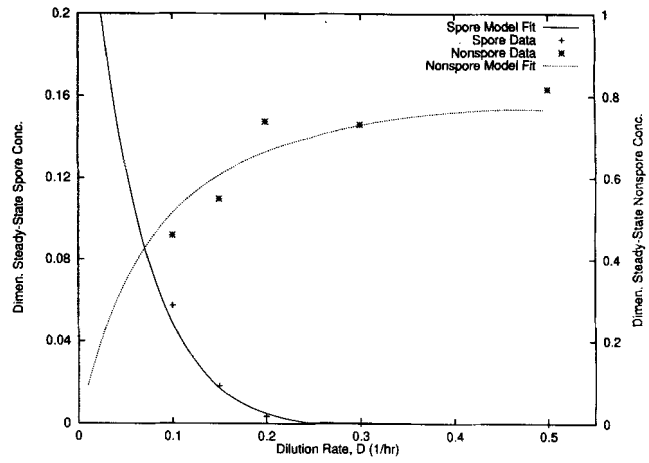

Figure 9. Steady-state spore and nonspore concentrations vs. dilution rate.

els. The system was considered at steady state when the biomass and substrate concentration measurements remained constant for a period of approximately 12 h. For a typical run, steady state was achieved approximately 24 h after continuous feeding began. After taking several samples for a given steady state, the feed flow rate was adjusted to a new flow rate, and the fermentor was allowed to adjust to a new steady state. Since the kinetics of spore formation are subject to a substantial time delay, the spore concentration consistently lagged the other states in achieving steady state. Steady-state substrate was not measured due to the fact that the substrate concentration was below measurable values for the glucose assay used in this study.

Accurate predictions of the steady-state biomass data were obtained with only minor adjustments to the model parameters. In particular, slight adjustments of the empirical sporulation initiation function provided good agreement between the predicted and experimental steady-state spore concentrations. The model fit to the steady-state spore and nonspore concentrations for dilution rates ranging from 0.1 to 0.5 (1/h) are shown in Figure 9. The model successfully predicts a decrease in spore concentration as dilution rate increases. Dawes and Thornley (1970) obtained a similar trend for steady-state spore-concentration-based dilution rates ranging from 0.05 to 0.38 (1/h).

Similar to the steady-state spore predictions, the segregated model does a good job of predicting steady-state nonspore biomass behavior. At low dilution rates, it appears that cell death and sporulation initiation are important processes, reducing levels of nonspore biomass at the low substrate conditions. As dilution rate increases, the availability of high substrate concentrations allows for increased vegetative populations.

Conclusions

This article outlines a structured-segregated model to describe growth and differentiation behavior of *B. licheniformis*. The model explicitly recognizes the three morphologically distinct cell types in a *Bacillus* culture, and acknowledges the age-segregated nature of the differentiating biomass. Using

batch and continuous-culture fermentations, parameter estimation techniques were utilized to identify the adjustable model parameters with confidence. The resulting model has been shown to track successfully growth and sporulation of both transient and steady-state cultures in a laboratory-scale fermentor.

A major motivation for modeling secondary-metabolite systems is to develop tools to aid in designing improved operating and control strategies. Considering that production of many secondary metabolites in bacteria and fungi are intimately linked to growth and differentiation, this model is a first step toward an overall growth and production model for *B. licheniformis*.

Notation

F_i = inlet-fermentor feed flow rate, 1/h
F_o = outlet-fermentor flow rate, 1/h
K_i = substrate internalization Michaelis constant, g/L
K_v = vegetative growth Michaelis constant, g/cell
s_c = critical substrate concentration needed to sustain growth, g/L
s_f = substrate feed concentration, g/L
y_g = germination yield coefficient, cells/g
y_s = sporulation yield coefficient, cells/g
α_g = maximum specific rate of spore germination, 1/h

Subscripts and superscripts

0 = initial condition
$'$ = derivative with respect to the sporangium age

Literature Cited

Bailey, J. E., and D. F. Ollis, *Biochemical Engineering Fundamentals*, 2nd ed., McGraw-Hill, New York (1986).

Bard, Y., *Nonlinear Parameter Estimation*, Academic Press, New York (1974).

Brenan, K. E., S. L. Campbell, and L. R. Petzold, *Numerical Solution of Initial-Value Problems in Differential-Algebraic Equations*, North-Holland, New York (1989).

Dawes, I. W., and J. H. M. Thornley, "Sporulation in *Bacillus subtilis*: Theoretical and Experimental Studies in Continuous Culture Systems," *J. Gen. Microbiol.*, **62**, 49 (1970).

Donohue, T. J., and R. W. Bernlohr, "Effect of Culture Conditions on the Concentrations of Metabolic Intermediates during Growth and Sporulation of *Bacillus licheniformis*," *J. Bacteriol*, **135**(2), 363 (1978).

Fordyce, A. P., "Modelling of Antibiotic Production by *Bacillus licheniformis* using a Structured/Segregated Approach," PhD Thesis, Univ. of Texas, Austin (1992).

Fredrickson, A. G., "Formulation of Structured Growth Models," *Biotech. Bioeng.*, **18**, 1481 (1976).

Hanlon, G. W., and N. A. Hodges, "Bacitracin and Protease Production in Relation to Sporulation During Exponential Growth of *Bacillus licheniformis* on Poorly Utilized Carbon and Nitrogen Sources," *J. Bacteriol.*, **147**(2), 427 (1981).

Jeong, J. W., J. Snay, and M. M. Ataai, "A Mathematical Model for Examining Growth and Sporulation Processes of *Bacillus subtilis*," *Biotech. Bioeng.*, **35**, 160 (1990).

Kramer, P. J., "An Analysis of the Major Metabolic Products of *Bacillus licheniformis* JF-2," Honors Thesis, Univ. of Texas at Austin (1990).

Lapidus, L., and G. F. Pinder, *Numerical Solution of Partial Differential Equations in Science and Engineering*, Wiley, New York (1982).

Losick, R., and L. Kroos, "Dependence Pathways for the Expression of Genes Involved in Endospore Formation in *Bacillus subtilis*," *Regulation of Procaryotic Development. Structural and Functional Analysis of Bacterial Sporulation and Germination*, Chap. 11, I. Smith, R. A. Slepecky, and P. Setlow, eds., American Society of Microbiology, Washington, DC, p. 223 (1989).

Losick, R., and P. Youngman, "Endospore Formation in *Bacillus*," *Microbial Development*, R. Losick and L. Shapiro, eds., Cold Spring Harbor Laboratories, Cold Spring Harbor, NY, p. 63 (1984).

Losick, R., P. Youngman, and P. J. Piggot, "Genetics of Endospore Formation," *Annu. Rev. Genet.*, **20**, 625 (1986).

Marahiel, M. A., W. Danders, M. Krause, and H. Kleinkauf, "Biological Role of Gramicidin S in Spore Functions," *Eur. J. Biochem.*, **99**, 49 (1979).

Nicholson, W. L., and P. Setlow, "Sporulation, Germination and Outgrowth," *Molecular Biology Methods for* Bacillus, Chap. 9, C. R. Harwood and S. M. Cutting, eds., Wiley, New York, p. 391 (1990).

Ollis, D. F., "A Simple Batch Fermentation Model: Theme and Variations," *Ann. N.Y. Acad. Sci.*, **413**, 144 (1983).

Ramkrishna, D., "Statistical Models of Cell Populations," *Adv. Biochem. Eng.*, **11**(1), 1 (1979).

Ramkrishna, D., A. G. Fredrickson, and H. M. Tsuchiya, "Dynamics of Microbial Propagation: Models Considering Inhibitors and Variable Cell Composition," *Biotech. Bioeng.*, **9**, 129 (1967).

Randolph, A. D., and M. A. Larson, *Theory of Particulate Processes*, 2nd ed., Academic Press, New York (1988).

Schaeffer, P., "Sporulation and the Production of Antibiotics, Exoenzymes, and Exotoxins," *Bacteriol. Rev.*, **33**(1), 48 (1969).

Schulz, V., R. Schorcht, Y. N. Ignatenko, Z. V. Sakharova, and M. P. Khovrychev, "Modellgestotzte Optimierung der Kontinuierlichen Fermentation von δ-Endotoxin," *Stud. Biophys.*, **107**(1), 43 (1985).

Shuler, M. L., S. Leung, and C. C. Dick, "A Mathematical Model for the Growth of a Single Bacterial Cell," *Ann. N.Y. Acad. Sci.*, **326**, 35 (1979).

Starzak, M., and R. K. Bajpai, "A Structured Model for Vegetative Growth and Sporulation in *Bacillus thuringiensis*," *Appl. Biochem. Biotechnol.*, **28/29**, 699 (1991).

Tsuchiya, H. M., A. G. Fredrickson, and R. Aris, "Dynamics of Microbial Cell Populations," *Adv. Chem. Eng.*, **6**, 125 (1966).

Villadsen, J., and W. Stewart, "Solution of Boundary-Value Problems by Orthogonal Collocation," *Chem. Eng. Sci.*, **22**, 1483 (1967).

Williams, F. M., "A Model of Cell Growth Dynamics," *J. Theor. Bio.*, **15**, 190 (1967).

Young, M., and J. Mandelstam, "Early Events During Bacterial Endospore Formation," *Adv. Microb. Physiol.*, **20**, 103 (1979).

Manuscript received Dec. 14, 1992, and revision received Apr. 29, 1996.